The Journal of Immunology

Localization on a Physical Map of the NKC-Linked *Cmv1* Locus Between *Ly49b* and the *Prp* Gene Cluster on Mouse Chromosome 6

Michael G. Brown, Jun Zhang, Ying Du, Janis Stoll, Wayne M. Yokoyama and Anthony A. Scalzo

J Immunol 1999; 163:1991-1999; ;
http://www.jimmunol.org/content/163/4/1991

The Journal of Immunology is published twice each month by
The American Association of Immunologists, Inc.,
1451 Rockville Pike, Suite 650, Rockville, MD 20852

Print ISSN: 0022-1767 Online ISSN: 1550-6606.

Localization on a Physical Map of the NKC-Linked *Cmv1* Locus Between *Ly49b* and the *Prp* Gene Cluster on Mouse Chromosome 6[1]

Michael G. Brown,[2]* Jun Zhang,* Ying Du,* Janis Stoll,* Wayne M. Yokoyama,* and Anthony A. Scalzo†

The *Cmv1* locus controls NK cell-mediated resistance to infection with murine CMV. Our recent genetic analysis of backcross mice demonstrated that the NK gene complex (NKC)-linked *Cmv1* locus should reside between the *Ly49* and *Prp* gene clusters on distal mouse chromosome 6. We have aligned yeast artificial chromosome (YAC) inserts in a contig spanning the interval between the *Ly49* and *Prp* gene clusters. This YAC contig includes 13 overlapping YAC inserts that span more than 2 megabases (Mb) in C57BL/6 (B6) mice. Since we have identified genomic clones that span the *Ly49-Prp* gene region, we hypothesize that at least one should contain the *Cmv1* locus. To narrow the *Cmv1* critical region, we developed novel NKC genetic markers and used these to genotype informative backcross and intra-NKC recombinant congenic mouse DNA samples. These data suggest that *Cmv1* resides on a single YAC insert within an interval that corresponds to a physical distance of ~390 kb. This high resolution, integrated physical and genetic NKC map will facilitate identification of *Cmv1* and other NKC-linked loci that regulate NK cell-mediated immunity. *The Journal of Immunology*, 1999, 163: 1991–1999.

Cytomegalovirus is a dsDNA virus that establishes chronic infection of its host that is characterized by latency and that persists throughout the lifetime of the host. Normally for the host, this viral infection is asymptomatic. However, latent CMV may reactivate and can lead to life-threatening complications in immunosuppressed or immunocompromised individuals. Human CMV (HCMV)[3] infection displays species-specific tropism, and thus it has not been possible to examine HCMV infection in easily manipulated experimental animals such as mice. Murine CMV (MCMV) displays many of the same molecular and pathologic features of HCMV infection, affording experimental analysis in a well-characterized animal model.

Although overall host resistance to MCMV is under multigenic control, regulation of acute viral burden within the spleen is determined by a single autosomal dominant locus designated *Cmv1* (1). The mouse *Cmv1* locus determines host mortality in different inbred strains following challenge with high titers ($\geq 10^5$ pfu) of MCMV. Moreover, NK cells are required for this *Cmv1*-dependent protective effect (2). Specifically, C57BL/6 (B6) mouse NK cells possess the *Cmv1*^{r} resistance allele, which limits splenic viral replication following low dose (10^3-5×10^4 pfu) MCMV infection. This directly correlates with B6 mouse survival rates following high dose MCMV challenge. In contrast, otherwise functionally competent BALB/c mouse NK cells are unable to limit splenic viral replication, and these MCMV-susceptible (*Cmv1*^{s}) mice do not survive high dose MCMV challenge.

Recently, the *Cmv1* locus was genetically mapped between the chromosome 6 *Ly49* and *Prp* gene clusters by analyzing segregation patterns of splenic viral titers in recombinant inbred (RI) and backcross mice following low dose MCMV challenge (2–4). The *Ly49* gene cluster is characteristic of several NK gene complex (NKC) gene clusters that are expressed predominantly in the NK cell lineage. *Ly49*, *Nkrp1*, *Cd94*, *Nkg2*, and *Cd69* genes encode NK cell receptors that are type II integral membrane proteins homologous to members of the C-type lectin superfamily (reviewed in Ref. 5). By contrast, the *Prp* gene cluster encodes proline-rich proteins that are expressed in mouse salivary glands (6). This gene cluster was used as an anchor locus for the original mapping of the NKC on mouse chromosome 6 (7, 8). Since the NKC-encoded NK cell receptors specifically recognize target cell ligands and modulate NK cell activity, they are good candidates to regulate NK cell activity in vivo.

Yeast artificial chromosome (YAC) inserts containing most of the known NKC-linked, NK cell-expressed genes have been identified and aligned in a contiguous array spanning more than 2 megabases (Mb) of the NKC with the *Ly49* cluster identified as the telomeric-most region (9, 10). Since our backcross analysis demonstrated that the *Cmv1* locus should reside in a distal region between the *Ly49* and *Prp* gene clusters, it was unlikely that we had previously identified *Cmv1*-containing YAC inserts. Therefore, we sought to identify NKC-linked YAC inserts that would span the critical region for the *Cmv1* locus.

*Rheumatology Division, Department of Medicine, Washington University School of Medicine, Howard Hughes Medical Institute, St. Louis, MO 63110; and †University of Western Australia, Nedlands, Western Australia, Australia

Received for publication March 24, 1999. Accepted for publication June 4, 1999.

The costs of publication of this article were defrayed in part by the payment of page charges. This article must therefore be hereby marked *advertisement* in accordance with 18 U.S.C. Section 1734 solely to indicate this fact.

[1] This work was supported in part by the Barnes-Jewish Hospital Research Foundation, by grants from the National Institutes of Health, and by the National Health and Medical Research Council of Australia (Grant 961305 to A.A.S.). M.G.B. was the recipient of a National Research Service Award from the National Institute of Allergy and Infectious Diseases. W.M.Y. is an investigator of the Howard Hughes Medical Institute. A.A.S. also received support from the Department of Industry, Science and Technology under the auspices of the Bilateral Science and Technology Collaboration Program.

[2] Address correspondence and reprint requests to Dr. Michael G. Brown, Division of Rheumatology, Box 8045, Washington University School of Medicine, 660 South Euclid Avenue, St. Louis, MO 63110. E-mail address: wylab03@imgate.wustl.edu

[3] Abbreviations used in this paper: HCMV, human CMV; MCMV, murine CMV; B6, C57BL/6; BAC, bacterial artificial chromosome; Mb, megabases; NKC, NK gene complex; PFGE, pulsed field gel electrophoresis; STS, sequence-tagged site; YAC, yeast artificial chromosome.

0022-1767/99/$02.00

Table I. *Characteristics of NKC STS and Southern probes used in this study*

Locus	Genbank Accession No.	Primers/Probe	Product/Probe Size (bp)	Primer Sequences (5′–3′)
Ly49b	U10304	BS289	1079	TAACTGGGTCAGTGTTGGTG
		BX446		CTGTTCTCTGTTGAGGTAGTG
D6Wum15	AF106670	109B5L.F2	135	TGACAGGAATAGAGACACAG
		109B5L.R2		GATCATTGTTCCCAAGAC
D6Wum18	AF11550	330B9L2.IF1	179	CTTCAAAGACAGAGAAGTGT
		330B9L2.IR1		TATTTGGAGAATCTTGTCCC
D6Wum16	AF106671	242D11L2.F1	337	GAATTCCTGATTTGATTT
		242D11L2.R1		CCTGTGGATACATCCCTAGA
Prp M14 (D6Mit13.1)	M23236	D6Mit13.1F	134	ATATGCTTCTGGCTAAAAGACCC
		D6Mit13.1R		CCTAACATGCTGAAAGGAAACA
				Southern Probe Source
Ly49b	U10304	Ly-49B	746	*Bst*XI/*Pst*I fragment of pLy49B
Prp Mp2[a]	M21462	Prp Mp2	893	*Xba*I fragment of pUMP2BE
D6Wum9	AF106665	200H7L	301	*Eco*RI fragment of p200Lts.5
D6Wum10	AF106666	79D7L	226	*Eco*RI/*Hin*dIII fragment of p79D7L
D6Wum12	AF106667	242D11L1	762	*Spe*I/*Eco*RI fragment of p242D11L1.S18
D6Wum13	AF106668	200H7R	658	*Eco*RI fragment of p200Rts.5
D6Wum14	AF106669	109F12R	244	*Eco*RI fragment of p109Rts.3
D6Wum15	AF106670	109B5L	175	*Eco*RI fragment of p109B5L.H5
D6Wum16	AF106671	242D11L2	349	*Eco*RI/*Hin*dIII fragment of p242D11L2.F1R1
D6Wum18	AF11550	330B9L2	388	*Eco*RI fragment of p330B9L2
D6Wum20	AF163323	392D6L2	793	*Xba*I fragment of p392D6L2.S7

[a] Prp Mp2 sequence was cloned from CD-1 mouse genomic DNA (20).

Interestingly, *Ly49b* (the most disparate *Ly49* gene member) does not reside in the *Ly49* gene cluster or anywhere in the previous NKC contig. Rather, we demonstrate here that *Ly49b* resides telomeric to the *Ly49* gene cluster. We have utilized YAC inserts containing the *Ly49b* gene together with those containing *Prp* genes to establish a YAC contig spanning the *Cmv1* locus. This distal NKC YAC contig spans more than 2 Mb of mouse chromosome 6 and could be aligned to the previous (proximal) NKC YAC contig. One or more of these YAC inserts should therefore contain the *Cmv1* locus. We have also developed novel NKC sequence-tagged site (STS) markers that were useful in genetic analysis of backcross and intra-NKC recombinant congenic inbred animals. Two of the novel NKC STS markers that were used in genetic analysis immediately flank the *Cmv1* locus. The genetic analysis suggests that *Cmv1* resides on a single NKC YAC insert in an interval that corresponds to a physical distance of ~390 kb.

Materials and Methods

YAC library screening

YAC clones were identified by screening the Whitehead Institute/MIT YAC libraries of *Eco*RI partially restricted B6 mouse DNA inserted into either the vector pYAC4 (the ymWIBR YAC library) or between the vectors pRML1 and pRML2 (the WI/MIT 820 YAC library (11, 12) (Research Genetics, Huntsville, AL) with NKC STS primers (Table I). YAC clone characteristics (i.e., size, stability, chimeric status, and number of transformant YACs) were assessed as described (9).

YAC clone DNA preparation and PCR analysis

Agarose plugs containing YAC clone DNA (~1×10^8 cells/plug) were prepared from yeast cells grown in selective media according to standard methods (13). For PCR analysis of YAC insert DNA, YAC clone DNA minipreps were prepared and tested by the PCR as described previously (9). For ^{32}P-PCR genotype analysis, forward primers were end labeled with [γ-^{32}P]ATP (sp. act. 3000 Ci/mmol; Amersham Life Science, Arlington Heights, IL) using T4 polynucleotide kinase (NEB, Beverly, MA) by standard methods (14). Labeled forward primers were used in PCR experiments as described for Mouse MapPairs (Research Genetics; Ref. 15). Labeled PCR products and [γ-^{32}P]ATP-labeled DNA m.w. Marker V (Boehringer-Mannheim, Indianapolis, IN) were visualized in acrylamide gels following denaturing PAGE.

Partial restriction of YAC DNA in agarose plugs and pulsed-field gel electrophoresis

Restriction of YAC DNA in agarose plugs was performed by standard methods (13). Pulsed-field gel electrophoresis (PFGE) was performed in either the CHEF DR II or the CHEF Mapper unit (Bio-Rad, Richmond, VA). Agarose plug DNA was separated in 1.0% chromosomal grade agarose (Bio-Rad) run in 0.5× TBE buffer (~14°C), using lambda concatemers (Bio-Rad) and yeast chromosomes (Bio-Rad) as size standards. Intact YAC clone DNA was separated by these PFGE conditions (6 V/cm, 120° angle, linearly ramped switching times from 50–90 sec for 20 h). For partially restricted YAC clone DNA, PFGE-ramped switching times were modified: typically, for larger YACs (>700 kb), switching times were ramped from 30–70 sec and for smaller YACs (<700 kb), switching times were ramped from 10–40 s.

Southern blots

For typing RFLP variants in inbred, recombinant inbred, backcross, and intra-NKC recombinant congenic inbred mice, 2–5 μg liver DNA samples (Mouse DNA Resource, The Jackson Laboratory, Bar Harbor, ME; Refs. (4 and 16) were restricted completely according to the manufacturer's conditions and electrophoresed on ~0.8% agarose gels. YAC clone DNA was prepared and separated as described above.

Southern blots were prepared and analyzed by standard methods (14). DNA was transferred onto Hybond-N membranes (Amersham Life Science) with 20× SSC. Southern probes labeled with [α-^{32}P]dCTP (Rediprime; Amersham Life Science) were hybridized to Southern blots. Stringent washing was performed in 0.2× SSC, 0.1% SDS at 58–62°C for typing RFLP Southern blots, and at 64–72°C for sequence-specific hybridization on YAC clone Southern blots.

YAC insert end clone isolation

pYAC4-modified YAC insert ends [designated (L) or (R) for pYAC4-left or -right arm-modified ends, respectively] were subcloned by the vectorette method (17), but with minor modification as described (9). Amplified products were subcloned into pBluescript II sk$^-$ (Stratagene, La Jolla, CA) and electroporated into *Escherichia coli*. pRML1- and pRML2-modified YAC insert ends (designated (L1) or (L2) for pRML1- or pRML2-modified ends, respectively) were subcloned by religation of *Xba*I-, *Spe*I-, or *Bam*HI-restricted YAC clone DNA and subsequent transformation into *E. coli*.

Table II. *Characteristics and NKC marker content of YAC inserts aligned to the distal NKC*

YAC Clone	Library[a]	Size[b] (kb)	Features[c]	NKC-Linked Markers[d]												
				Ly49a	*D6Wum5*	*D6Wum15*	*D6Wum13*	*D6Wum12*	*Ly49b*	*D6Wum14*	*D6Wum9*	*D6Wum10*	*D6Wum20*	*D6Wum18*	*D6Wum16*	*PrpMp2*	*D6Mit13.1*
52A6[e]	ymWIBR	530	S, CH$^-$	+	+	−	−	−	−	−	−	−	−	−	−	−	−
109B5[e]	ymWIBR	1000	U, CH$^-$	+	+	+	−	−	−	−	−	−					
109F12	ymWIBR	715	S, CH$^-$	−	−	+	+	+	+	+	−	−			−	−	
200H7	ymWIBR	660, 590, 530	U, CH$^-$	−	−	−	+	+	+	+	+	−			−	−	
86F9	ymWIBR	660, 595	U, ND	−	−	−			+	+		−					
76B10[f]	ymWIBR	1000, 960, 860	U, CH$^+$			−		−	−	+	+	−	−		−		
452H5	WI/MIT 820	≥1100	S, ND			+		+	+		+	+	−		−		
79D7	ymWIBR	475, 360, 200	U, ND			−		+	+	+	+	+	−	−	−	−	−
242D11	WI/MIT 820	820	S, CH$^-$					+	+			+	+	+	+	+	−
392D6	WI/MIT 820	1130, 1100	U, ND									−	+	+	+	+	+
330B9	WI/MIT 820	970	S, ND									−	−	+	+	+	+
377D10	WI/MIT 820	930, 830	U, ND									−	−		+	+	+
289D8	WI/MIT 820	ND	ND												−	+	+
289D9	WI/MIT 820	ND	ND												−	+	+
144B3	WI/MIT 820	ND	ND												−	+	+

[a] Two different Whitehead YAC libraries have been screened using NKC STS markers (see *Materials and Methods*).
[b] Size of pulsed-field gel bands was determined by Southern analysis using YAC vector and NKC Southern probes.
[c] S, stable; U, unstable; ch$^+$, nonchimeric; ch$^+$, chimeric; ND, not determined.
[d] NKC STS primers and/or Southern probes were used to assess the content of these NKC YAC clones (Table I). Positive (+) and negative (−) results are indicated. Some YAC clones were not tested with some NKC markers.
[e] Proximal NKC marker content and characteristics for these YAC clones were reported previously (9).
[f] Chimerism of this clone has been inferred since the left end probe subcloned from this YAC insert does not overlap other NKC YACs.

Transformants were identified by pRML1- and pRML2-specific colony PCR using pRML1-specific primers pRML1.F2, 5′-GAATGTTACCAC CTAAATAAG-3′, and pRML1.R1, 5′-AGTGAGGGTTAATTT-ACG TAG-3′; or pRML2-specific primers pRML2.F2, 5′-GACAAGAAAAG CAGATT-AAATAG-3′, and pRML2.R1, 5′-AATTCGATGTACCCAATT CGC-3′. T7, T3, SK, KS, pRML1.F2, pRML2.F2, and NKC STS primer extension products were sequenced using the ABI Prism Dyedeoxy termination kit (Perkin-Elmer, Foster City, CA) to verify YAC insert ends. Sequence analysis was performed using the Sequencher 3.0 program (Gene Codes, Ann Arbor, MI). YAC insert end probes were also assessed on Southern blots of YAC and mouse genomic DNA restricted with frequently cutting restriction enzymes.

YAC vector Southern probes

pYAC4 vector arm probes were as described (9). pRML1 and pRML2 unique sequences were subcloned as follows: The pRML1- and pRML2-specific amplified products from the respective vectors were TA subcloned into the *Eco*RV site of pBluescript II sk$^-$ as described (9). The 266-bp *Eco*RI/*Hin*dIII fragment of pBSRML1 and the 238-bp *Eco*RI/*Hin*dIII fragment of pBSRML2 were used as Southern probes. Probes were gel purified (Prep-A-Gene; Bio-Rad) and were subsequently verified and quantitated by agarose gel electrophoresis.

Results

Previously, we identified and aligned YAC inserts that contained *Nkrp1*, *Ly49*, and *Cd94/Nkg2* gene clusters but did not contain the *Ly49b* or *Prp* genes (9). *Ly49b*-containing YAC inserts were identified using *Ly49b*-specific oligonucleotides (Tables I and II) and positioned between the *Ly49* and *Prp* gene clusters (see below). Although B6 mouse YAC clones containing *Prp* gene cluster microsatellites had been identified previously, they had not been further characterized (15, 18, 19). Since *Cmv1* was genetically mapped between *Ly49a* and the *Prp* gene cluster previously (4), we sought to identify a complete set of overlapping genomic clones that would span this NKC region and potentially contain the *Ly49b* gene.

Analysis of the Ly49b region

Initially, YACs containing *Ly49b* genes were characterized by restriction mapping and STS content analysis. *Ly49b*-containing YACs (Table II) were *Mlu* I restriction mapped by Southern analysis of DNA that had been separated by PFGE. A representative composite was produced of *Mlu*I-restricted YACs 109F12 and 200H7 on the same nylon membrane successively hybridized with six different Southern probes (Fig. 1*A*). Notably, the Ly-49B cDNA hybridized strongly with a 200-kb *Mlu*I fragment and weakly with a smaller *Mlu*I fragment from both YAC inserts. This probe did not hybridize with the *Ly49a* gene-containing YAC insert 52A6 or other 109F12 and 200H7 *Mlu*I fragments that were also on the nylon membrane (not shown). These results confirmed the location of *Ly49b* on YACs 109F12 and 200H7 (Fig. 1*B*) that did not contain the *Ly49a* gene.

Subsequent successive hybridizations with YAC insert end probes 109F12R, 200H7R, and 200H7L were performed so that placement of *Mlu*I sites on these YAC inserts could be completed (Fig. 1*A*). Curiously, probe 200H7R hybridized with more than one fragment of each insert, but not YAC insert 52A6. This probe may contain DNA sequence elements that are common, but restricted, to this NKC region. The 200H7L probe did not hybridize with YAC 109F12 fragments, demonstrating that this locus does not reside on 109F12. Importantly, these left and right YAC end probes hybridized with those fragments also identified by the appropriate YAC vector probes. Similarly, YAC inserts 79D7 and 242D11 could also be aligned to the *Ly49b* contig by their NKC STS marker content and *Mlu*I and *Sal*I restriction profiles (Table II, Fig. 1*B*). Although YACs 452H5, 86F9, and 76B10 also could

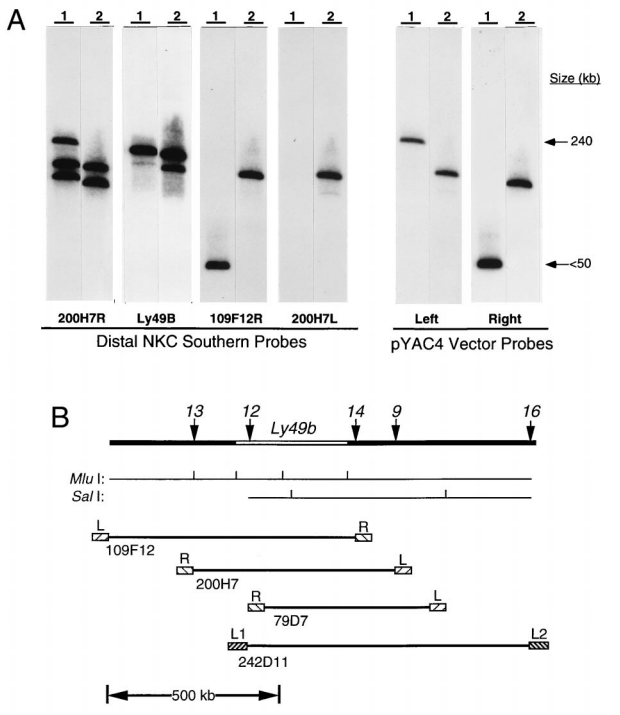

FIGURE 1. A physical map of the *Ly49b* NKC region. *A*, Agarose plugs containing YAC clones 109F12 (*lane 1*) and 200H7 (*lane 2*) were partially (not shown) and completely restricted with *Mlu*I, separated by PFGE, and Southern blotted. YAC clone 52A6 was included as a NKC control DNA (not shown). PFGE lanes from this Southern blot containing completely restricted YAC clone DNA and probed successively with six different probes (as indicated) are shown. *B*, At *top*, the *Ly49b* region on mouse chromosome 6 is depicted. Positions of the NKC STS markers *D6Wum13*, *D6Wum12*, *D6Wum14*, and *D6Wum9* are indicated on the chromosome map. *Below* the chromosome map, an *Mlu*I restriction site map for this NKC interval is shown. *Sal*I sites that were mapped on YACs 79D7 and 242D11 are also shown. *Below* the restriction maps, an alignment of YAC inserts 109F12, 200H7, 79D7, and 242D11 are shown. YAC insert orientation to the contig is indicated by the designated YAC ends: pYAC4R (R), pYAC4L (L), pRML1 (L1), or pRML2 (L2). The *Ly49b* interval (open bar) resides between the mapped *Mlu*I sites as indicated.

be aligned to or near the *Ly49b* region based on STS marker content analysis (Table II), these YAC inserts have not been extensively mapped.

Importantly, a genetic analysis could be performed to confirm and extend these physical findings because the 200H7L Southern probe identified an RFLP (*D6Wum9*) that distinguishes B6 and BALB/c alleles for this locus. *D6Wum9* genotypes of the backcross mice (BALB/c × C57BL/6)F_1 × BALB/c No. 37 and (A/J × C57BL/6)F_1 × A/J No. 44 and several of the intra-NKC recombinant congenic mice (BALB.B6-*Cmv1*^{r}(CT 1–18)) confirmed an NKC location for *D6Wum9* distal to the *Nkrp1* and *Cd69* genes (Tables III and IV). Likewise, *D6Wum9* genotype analysis of the backcross mouse panels and the intra-NKC recombinant congenic mice confirmed the NKC location for *D6Wum9* proximal to the *Prp* gene cluster. Overall, these analyses confirmed the alignment of the *Ly49b*-containing YACs to the NKC region between *Ly49a* and the *Prp* gene cluster.

Analysis of the Prp *region*

Likewise, YACs containing *Prp* genes were restriction mapped with several enzymes and subsequent Southern analysis using probes for the *Prp Mp2* gene (20), YAC insert ends 392D6L2 and 242D11L2, and pRML1 and pRML2 YAC vectors (Fig. 2*A*). The *Prp Mp2* probe hybridized with 330B9 and 392D6 fragments, but not 52A6 or 242D11 YAC inserts. Although the pRML1 probe may weakly hybridize with a single yeast chromosome sequence in all of the YAC clones tested, it also specifically hybridizes with single restriction fragments from each YAC insert (Fig. 2*A*). Importantly, *Prp* and pRML1 probes both hybridized with the same size *Bss*HII fragment of 330B9, suggesting that the *Prp Mp2* gene resides near the pRML1 end of this YAC insert. An internal 392D6 *Bss*HII fragment hybridizes with the *Prp Mp2* probe since it does not hybridize with either of the YAC vector probes, pRML1 or pRML2. Curiously, the *Prp* gene-containing 392D6 *Mlu*I fragment is smaller than the corresponding 330B9 *Mlu*I fragment, although the *Prp* gene-containing 392D6 *Bss*HII fragment is larger than the corresponding 330B9 *Bss*HII fragment. Thus, YAC 392D6 may contain a rearranged or partially deleted DNA insert, or a 330B9 *Mlu*I site may have been altered. Nevertheless, members of the *Prp* gene cluster were mapped to the pRML1 end of YAC 330B9, and this fragment overlaps an internal *Bss*HII fragment of 392D6. This probe may be detecting more than a single gene from the *Prp* cluster since it hybridized with two similarly sized, *Sal*I fragments of each YAC and since this *Prp Mp2* exon 2 genomic probe does not contain an internal *Sal*I site (Fig. 2*A*; Ref. 20). Moreover, these YAC inserts were specifically amplified by *Prp M14* gene-specific primers (Table II). Southern analysis with a pRML2 vector probe confirmed that *Prp* genes do not reside on the pRML2-modified ends of these inserts (Fig. 2*A*). By this analysis, YACs 392D6 and 330B9 could be mapped and aligned in a *Prp* gene cluster YAC contig (Fig. 2*B*).

Overlap of Ly49b, Prp, and the proximal NKC regions

Notably, the 242D11L2 Southern probe hybridized with the pRML2-modified YAC insert ends of YACs 242D11, 330B9, and 392D6 (Fig. 2*A*). Note that *Sal*I fragments were not detected by the pRML2 vector probe since this vector contains a *Sal*I site that resides very close to the vector cloning site for mouse insert DNA. Hence, this end of the *Ly49b*-containing YAC contig (*D6Wum16*) must reside between the L2-modified ends of 330B9 and 392D6 and the adjacent *Sal*I site on each of these clones. In support of this alignment, *D6Wum16*-specific oligonucleotides amplified the expected 337-bp product from YAC 242D11 and three of four *Prp* containing YAC inserts that were tested, while other NKC YACs were not amplified (Table II). *D6Wum18*-specific oligonucleotides specifically amplified YACs 330B9, 392D6, and 242D11 (Table II). Southern probe 392D6L2 (*D6Wum20*) hybridized with the L2-modified ends of YACs 392D6 and 242D11, but did not hybridize with YACs 52A6 or 330B9 (Fig. 2*A*). Finally, a bacterial artificial chromosome (BAC) insert (~65 kb) that contains both *D6Wum18* and *D6Wum16* has been identified (M. G. Brown, J. Stoll, and W. M. Yokoyama, unpublished data). Taken together, the results suggest that the order for these NKC STS markers is *D6Wum20-D6Wum18-D6Wum16* on YAC 242D11 and that *D6Wum18* and *D6Wum16* should each reside within 65 kb of the other. These findings therefore confirmed the alignment of the *Ly49b*-containing YAC contig with the *Prp*-containing YAC contig into an overall distal NKC YAC contig. More importantly, since *D6Wum9*, *D6Wum12*, and *D6Wum13* must reside centromeric to *D6Wum16* and the *Prp* gene cluster (Tables III and IV), these data provided orientation of this contig on mouse chromosome 6.

To determine whether this distal NKC YAC contig could be aligned with the previously established NKC proximal YAC contig, we surveyed selected YAC clones with the 109B5L Southern probe (*D6Wum15*), the telomeric-most STS marker from the proximal contig. Importantly, this probe hybridized with YACs 109B5

Table III. *Genotype analysis of informative backcross mice with novel NKC STS markers*

Locus	(BALB/c × C57BL/6J)F_1 × BALB/c Mice																			
	2	3	6	7	9	13	16	21	31	32	34	35	36	37	39	40	44	46	52	54
Nkrp1[a]	b[b]	b	b	b	b	b	c	c	b	b	c	b	c	c	b	c	b	c	b	c
Cd69	b	b	b	b	b	b	c	c	b	b	c	b	c	c	b	c	b	c	b	c
Ly49a	b	b	b	b	b	b	c	c	b	b	c	b	c	b	b	c	b	c	b	c
D6Wum15[c]	b	b	b	b	b	b	−	−	b	b	−	b	−	b	b	−	b	−	b	−
D6Wum13[d]	b	b	b	b	b	b	c	c	b	b	c	b	c	b	b	c	b	c	b	c
D6Wum9[d]	b	b	b	b	b	b	c	c	b	b	c	b	c	b	b	c	b	c	b	c
Cmv1	b	b	b	b	b	b	c	b	b	b	c	b	c	b	b	c	b	c	b	c
D6Wum16[c]	b	b	b	c	b	b	c	b	b	b	c	b	c	b	c	c	b	b	c	c
Prp	b	b	b	c	b	b	c	b	b	b	c	b	c	b	c	c	b	b	c	c

Locus	(A/J × C57BL/6J)F_1 × A/J Mice										
	4	16	17	18	21	28	29	31	44	47	53	56
Nkrp1	a	a	b	b	a	b	a	b	a	b	b	a
Ly49a	a	a	b	b	a	b	a	b	b	b	b	a
D6Wum15[c]	−	−	b	b	−	b	−	b	b	b	b	−
D6Wum13	a	a	b	b	a	b	a	b	b	b	b	a
D6Wum9[d]	a	a	b	b	a	b	a	b	b	b	b	a
Cmv1	a	a	b	b	a	b	b	b	b	b	b	a
Prp	a	a	b	b	a	b	b	b	b	b	b	a

[a] *Nkrp1, Cd69, Ly49a, Cmv1,* and *Prp* alleles in these mice have been reported previously (4).
[b] For the recombinant chromosome, b = B6 allele, c = BALB/c allele, and a = A/J allele. For the *Cmv1* locus, b = *Cmv1*^{r} and a and c = *Cmv1*^{S}.
[c] B6 dominant alleles were determined using radiolabeled NKC locus-specific primers (Table I). *D6Wum15*-specific primers do not amplify a product from the BALB/c or A/J genomes ((−); and see Table IV). *D6Wum16*-specific primers amplify a minor product of identical size from the B6 and BALB/c genomes in addition to the expected, major product.
[d] *D6Wum13* and *D6Wum9* alleles were determined by restriction of backcross mouse DNA and Southern hybridization with the 200H7R and 200H7L Southern probes, respectively (Table I). The 200H7R probe detects 4.8-kb B6 and 5.5-kb BALB/c or A/J *Hin*dIII fragments. The 200H7L probe detects 2.5-kb and 3-kb B6 and 3.5-kb BALB/c or A/J *Hin*dIII fragments.

and 109F12 (a *Ly49b*-containing YAC) but not other NKC-aligned YAC inserts (Table II). In addition, probe 109B5L hybridization with the Southern blot represented in Fig. 1*A* revealed specific detection of the pYAC4L-modified *Mlu*I fragment (240 kb) of YAC 109F12 (data not shown). Moreover, this locus was confirmed on YACs 109B5, 109F12, and 452H5 (Tables I and II) and was found to be tightly linked with the *Ly49* genes and the distal NKC marker *D6Wum9* (Tables III and IV) using radiolabeled 109B5L-specific oligonucleotides. Thus, these results facilitated the alignment and orientation of the proximal and distal NKC YAC contigs to a region on mouse chromosome 6 that includes the *Cmv1* locus.

Assignment of the Cmv1 *critical region on the NKC physical map*

In our previous backcross analysis in mice, *Cmv1* was genetically mapped to a 0.5-cM interval between the *Ly49* and *Prp* gene clusters, but its physical location could not be identified since the physical interval between *Ly49* and *Prp* had not been characterized (4). From the current physical map, this region extends beyond 2 Mb,

Table IV. *Genotype analysis of intra-NKC recombinant congenic mouse strains*

Locus	Intra-NKC Recombinant Congenic BALB.B6-CT 1–18 Mouse Strains[a]																	
	1	2	3	4	5	6	7	8	9	10	11	12	13	14	15	16	17	18
Nkrp1[b]	c[c]	c	c	c	c	b	c	b	c	c	c	b	c	c	c	c	c	c
Cd69	c	c	c	c	c	b	c	b	c	c	c	b	c	c	c	c	c	c
Cd94	c	b	b	b	c	c	b	b	c	b	c	b	b	b	b	c	c	c
D6Wum4[d]	c	b	b	b	c	c	b	b	c	b	c	b	b	b	b	c	c	c
Ly49a	c	b	b	b	c	c	b	b	c	b	c	b	b	b	b	c	c	c
D6Wum15[e]	−	b	b	b	−	−	b	b	−	b	−	b	b	b	b	−	−	−
D6Wum12[d]	c	b	b	b	c	c	b	b	c	b	c	b	b	b	b	c	c	c
D6Wum9[d]	c	b	b	b	c	c	b	b	c	b	c	b	b	b	b	c	c	c
Cmv1	c	b	b	b	c	c	b	b	c	b	c	b	b	b	b	c	c	c
D6Wum16[e]	b	b	b	b	b	c	b	b	c	b	b	c	c	c	c	b	b	b
D6Mit13	b	b	b	b	b	c	b	b	c	b	b	c	c	c	c	b	b	b

[a] Intra-NKC recombinant mouse strains were derived from the BALB.B6-*Cmv1*^{r} congenic strain as described previously (16).
[b] *Nkrp1, Cd69, Cd94, Ly49a, Cmv1,* and *D6Mit13* (*Prp*) alleles in these mice have been reported previously (16).
[c] Allele designations were as described in Table III.
[d] *D6Wum4, D6Wum12,* and *D6Wum9* alleles were determined by restriction of intra-NKC recombinant mouse DNA and Southern hybridization with 52R (9), 242D11L1, and 200H7L probes, respectively (Tables I and II). The 242D11L1 probe detects 4-kb and 6-kb B6 fragments and 3-kb and 4-kb BALB/c or A/J *Bgl*II fragments.
[e] Allele determinations were as described in Table III.

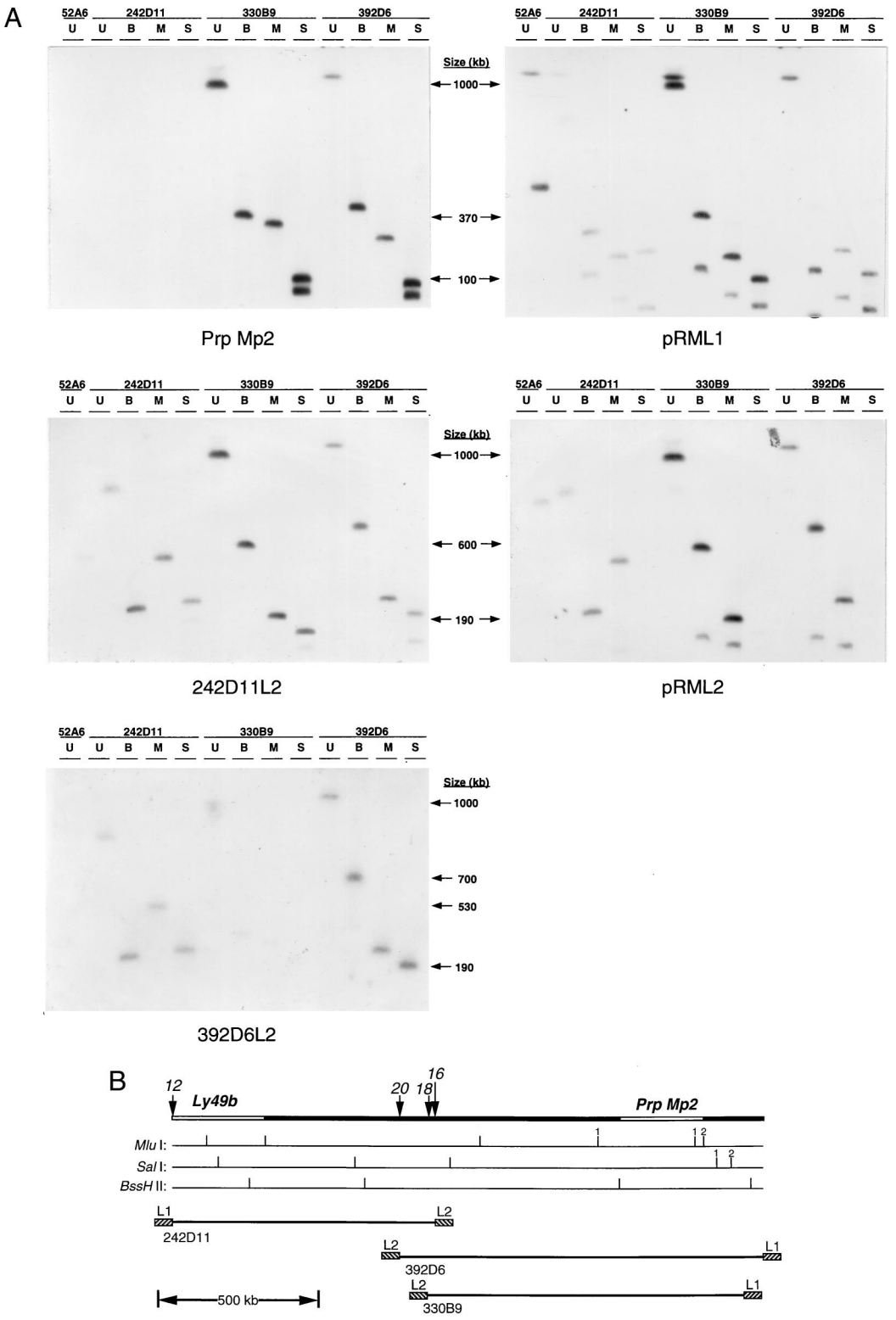

FIGURE 2. A physical map of the *Prp Mp2* gene cluster region of mouse chromosome 6. Agarose plugs containing YAC clones 242D11, 330B9, and 392D6 were completely restricted with *Bss*HII (B), *Mlu*I (M), and *Sal*I (S). Restricted and uncut (U) DNA samples, including YAC clone 52A6, were separated by PFGE and Southern blotted. *A*, The Southern blot was probed with a Prp Mp2 exon 2 probe (20), YAC end probes 242D11L2 and 392D6L2 (Table I), and YAC vector probes pRML1 and pRML2, as designated. Restriction fragment sizes were determined by comparison with yeast chromosome and lambda concatemer mobilities in PFGE. Note that pRML1 weakly hybridized with *Bss*HII (~110 kb), *Mlu*I (~80 kb), and *Sal*I (~40 kb) fragments of a yeast chromosome. *B*, At *top*, depicted is the mouse chromosome 6 *Prp* region. Positions for *D6Wum12, -20, -18,* and *-16* are shown. *Below* the chromosome map, *Bss*HII, *Mlu*I, and *Sal*I restriction sites that have been mapped are shown. Note that additional internal *Bss*HII sites on YAC 242D11 and internal *Mlu*I and *Sal*I sites on YACs 392D6 and 330B9 may exist that were not mapped by this analysis. Discrepant 330B9 (1) and 392D6 (2) *Mlu*I sites are indicated. *Below* the *Prp* region restriction maps, an alignment of YAC inserts 242D11, 392D6, and 330B9 is shown. An interval for the *Prp* gene cluster (open bar) bounded by the proximal *BssH*II and distal *Mlu*I sites is also shown. YAC insert orientation to the contig is indicated as described for Fig. 1*B*.

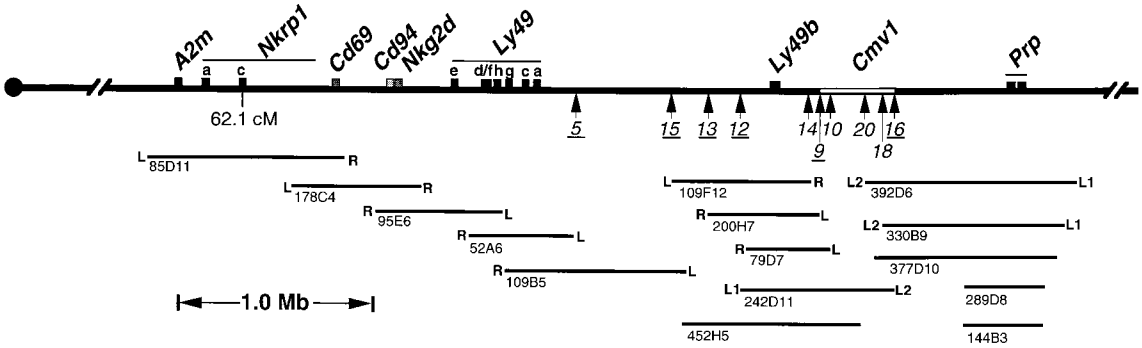

FIGURE 3. Alignment of the C57BL/6 mouse NKC proximal and distal YAC contigs spanning the *Cmv1* locus. At *top*, mouse chromosome 6 and positions of the proximal NKC gene clusters, *Ly49b*, and the *Prp* gene cluster are shown (centromeric-telomeric, respectively). An approximate position for *D6Wum15* is shown between the pYAC4L (L) end of YAC 109F12 and the 109F12 adjacent distal *Mlu*I site. Proximal (*D6Wum9*) and distal (*D6Wum16*) NKC boundaries for the *Cmv1* critical region (open bar) on the physical map are shown. Novel NKC STS markers (*D6Wum*) are shown *below* the chromosome map. NKC STS markers that distinguish different alleles in inbred mouse strains are underlined. At *bottom*, an overall NKC YAC contig is shown from which the physical map was established (not all of the NKC aligned YAC inserts are shown). YAC insert orientation to the contig is indicated as described for Fig. 1*B*.

spanning several YAC clone inserts. We therefore attempted to determine the location of the *Cmv1* genetic interval on the NKC physical map before embarking on a gene-screening strategy that would require investigation of multiple large YAC inserts.

Initially, we genotyped backcross and intra-NKC recombinant congenic inbred mice for *D6Wum9* alleles (Tables III and IV). Although no animals that contained recombination breakpoints between *Ly49a* and *D6Wum9* were identified, two of the backcross animals contained breakpoints between *D6Wum9* and *Cmv1*. (BALB/c × C57BL/6)F_1 × BALB/c mouse No. 21 and (A/J × C57BL/6)F_1 × A/J mouse No. 29 contained BALB/c or A/J *D6Wum9* alleles, respectively, but each animal contained a B6 *Cmv1*^{r} allele. Hence, *D6Wum9* resides proximal to the *Cmv1* locus, thus providing a new centromeric NKC boundary for *Cmv1*. Likewise, we genotyped the animals described above with *D6Wum16*. Notably, the *D6Wum16* alleles matched the *Prp* gene alleles in all of the animals tested from each genetic panel (Tables III and IV). Thus, the data support the conclusion that *D6Wum16* resides distal to the *Cmv1* locus, and therefore *D6Wum16* should serve as a novel telomeric boundary for the *Cmv1* genetic interval.

From the STS content mapping of genomic clones, it was apparent that the *Cmv1* flanking markers *D6Wum9* and *D6Wum16* reside on YAC 242D11 (Table II). In the alignment of YAC 242D11 with other YAC inserts from the distal NKC contig, the 200H7 telomeric-most *Mlu*I site should correspond to the 242D11 telomeric-most *Mlu*I site. In support of this alignment, the 200H7L probe hybridized specifically with the pYAC4L-modified 200H7 *Mlu*I fragment (~140 kb) and the pRML2-modified 242D11 *Mlu*I fragment (~530 kb), but not with the smaller pRML2-modified 242D11 *Sal*I or *Bss*HII fragments (Fig. 1, *A* and *B*, and data not shown). Thus, *D6Wum9* resides ~140 kb distal to this *Mlu*I site on YACs 200H7 and 242D11 and the *D6Wum9–16* physical interval should span ~390 kb. Since these *Cmv1*-flanking STS markers both reside on YAC 242D11, we conclude that 242D11 should contain the *Cmv1* locus and that the *Cmv1* critical region corresponds to a maximum physical distance of ~390 kb on this YAC insert.

Discussion

In this report, we have identified, mapped and aligned thirteen new YAC inserts to the NKC on mouse chromosome 6. Overlap of these novel NKC YAC inserts with the adjacent, previously established proximal NKC YAC contig expanded the NKC coverage (*A2m-Prp*) from ~2.5 Mb to ~4.7 Mb and includes 27 YAC inserts in total, corresponding to a 0.7-cM genetic interval (Fig. 3). Since *D6Wum15* resides somewhere on the ~240-kb pYAC4L-modified *Mlu*I fragment of YAC 109F12, and since the distance between *D6Wum18* and *D6Wum16* is ≤65 kb, the overall physical size estimate for the aligned proximal and distal NKC YAC contigs may be ±310 kb. Using the YAC contig as a backbone, we have physically mapped most known NKC-linked, NK cell-expressed genes and the *Prp* gene cluster. Recently, McQueen and coworkers identified and mapped five novel *Ly49* genes, four of which clearly reside in the *Ly49* gene cluster (21). In accord with the data presented here, these genes do not overlap the *Ly49b* region (21). Conceivably, the NKC could extend beyond the overall YAC contig reported here to include additional gene products that are structurally and/or functionally related to previously reported NKC members (5).

Notably, the new distal NKC YAC contig spans the original NKC genetic interval containing *Cmv1*. Nine novel NKC locus-specific markers, including five that distinguish different inbred mouse alleles, have been positioned on the NKC physical map in this study, including genetic markers that flank the *Cmv1* locus. The previous *Cmv1* critical region (>2 Mb) now has been narrowed to a fragment of a single YAC insert that corresponds to a physical distance of ~390 kb. This clone should contain the *Cmv1* locus, but YACs may be prone to DNA rearrangements and partial deletions. However, we have aligned more than one genomic clone to this NKC region, thus providing multiple coverage to validate the physical map. As an alternative approach, we are now aligning BAC inserts to the *Cmv1* critical region and preliminary data corroborates this map. Therefore, we have identified novel NKC-linked genetic markers that enabled us to narrow the *Cmv1* locus to an NKC region included on individual genomic clones.

Genetic localization of *Cmv1* on the physical map was inherently reliant upon analysis of intra-NKC recombinant mice, especially two informative backcross mice [(BALB/c × C57BL/6)F_1 × BALB/c mouse No. 21 and (A/J × C57BL/6)F_1 × A/J mouse No. 29], one from each backcross panel containing a recombination breakpoint between *D6Wum9* and the *Cmv1* locus (Table III). Importantly, each of these animals was resistant to MCMV infection but contained BALB/c or A/J alleles for proximal NKC markers and the distal NKC marker *D6Wum9*, respectively. Hence, recombination breakpoints in these animals should have resided

between *D6Wum9* and *Cmv1*. Although similar recombinant animals were not identified by Depatie and coworkers or in our intra-NKC recombinant congenic mice (Refs. 16 and 22; and see Table IV), our backcross data are not inconsistent, since it is possible that the additional genetic approaches may have failed to generate animals containing similar low frequency recombination events. In light of this, it is interesting that most of the intra-NKC recombinant backcross mice (six of eight) and four of the original 12 intra-NKC recombinant mouse strains (BALB.B6-CT 1–12) contain breakpoints within the *D6Wum9-D6Wum16* (~390 kb) NKC interval. During production of homozygous stock for these "CT" strains, six additional independent intra-NKC recombinant congenic mice (CT 13–18) were identified that are also recombinant in this narrow NKC region (Ref. 16; Table IV). Moreover, half of the original intra-NKC recombinant congenic "CT" mice (6 of 12) and the intra-NKC recombinant mouse strain B6.BALB-TC1 that was derived from the B6.BALB-*Cmv1*^{s} congenic strain are recombinant within an ~500-kb interval of the proximal NKC between the *Cd69* and *Cd94* genes (Ref. 16; Table IV). This suggests 1) that two NKC regions, one in the proximal NKC between *Cd69* and *Cd94*, and the other in the distal NKC between *D6Wum9* and *D6Wum16*, may be recombinogenic, and 2) that *Cmv1* should reside between boundaries defined by the recombination breakpoints identified in two sets of distal NKC recombinant mice, those that are recombinant between *D6Wum9* and *Cmv1* and those that are recombinant between *Cmv1* and *D6Wum16*. The recombination hotspots flanking multiple NKC gene clusters that can modulate NK cell function may provide a means to exchange NKC "haplotypes" during meiotic recombination. These haplotypes are predicted to consist of a large number of genes that display polymorphism and influence NK cell function and that segregate with each other. As such, the functions of individual genes may be dependent on alleles in other linked genes.

In this analysis, we also identified the precise *Mlu*I fragments of different YAC inserts that hybridize with the Ly-49B cDNA. Because this probe also hybridizes weakly to an additional *Mlu*I fragment of both YAC inserts, the *Ly49b* gene may contain an *Mlu*I site. Alternatively, the Ly-49B cDNA may be hybridizing with one or more *Ly49b*-like genes. We hypothesize that such a gene(s) would be *Ly49b* related since this probe does not hybridize with the *Ly49* gene cluster-containing YAC inserts. Hence, an additional gene cluster may reside in the NKC ~1 Mb distal to the *Ly49* gene cluster. Importantly, none of the *Ly49* genes, including the *Ly49b* gene, should be considered a *Cmv1* candidate gene since the *Ly49-D6Wum9* linkage group segregated from the *Cmv1* locus in the genetic analysis of the backcross mice. On the other hand, a gene related to *Ly49b* could be a relevant candidate since the *Cmv1* genetic interval is immediately distal to the *Ly49b* NKC region and the NKC contains several clusters of highly related genes (9, 10, 23).

Likewise, we have physically mapped the *Prp Mp2* gene to a presumed telomeric physical boundary for the NKC. This region resides ~2.5 Mb from the *Ly49* gene cluster and also appears to contain multiple genes that hybridize with the Prp Mp2 Southern probe. This is not a surprising result given that the mouse *Prp* gene cluster may contain several different genes that encode proline-rich proteins expressed in the salivary glands of mice (6). For the purposes of this work, *Prp* gene mapping provided an initial physical boundary for the *Cmv1* genetic interval.

Ultimately, this physical map and the novel NKC locus markers that have been derived from it should facilitate positional gene cloning strategies not only for *Cmv1*, but also for other NKC-linked loci that are defined by immunological phenotypes. These immune function regulators include loci that affect mouse resistance to ectromelia (*Rmp1*) and possibly also to *Leishmania*, loci that modulate natural killing of xenogeneic target cells (*Chok*), and loci that affect non-insulin-dependent diabetes mellitus susceptibility and *Bordetella pertussis*-induced histamine sensitization (24–30). The mouse NKC may also contain an orthologue of the rat *Nka* locus that regulates NK cell-mediated alloreactivity (31). Moreover, the resources described herein should prove invaluable for the localization of these and other mouse chromosome 6 loci that are tightly linked to the NKC, including the *Soa* locus that affects taste discrimination in mice (32). We suspect that the NKC may also contain genes that have yet to be identified. Hence, this report will provide the framework for the identification of additional NKC-linked genes and regulatory elements that are critical for immune functions.

Acknowledgments

We thank D. M. Carlson for kindly providing the pUMP$_2$BE plasmid. We also thank J. Heusel, B. Plougastel, and E. Ho for critical review of the manuscript.

References

1. Scalzo, A. A., N. A. Fitzgerald, A. Simmons, A. B. La Vista, and G. R. Shellam. 1990. *Cmv-1*, a genetic locus that controls murine cytomegalovirus replication in the spleen. *J. Exp. Med. 171:1469.*
2. Scalzo, A. A., N. A. Fitzgerald, C. R. Wallace, A. E. Gibbons, Y. C. Smart, R. C. Burton, and G. R. Shellam. 1992. The effect of the *Cmv-1* resistance gene, which is linked to the natural killer cell gene complex, is mediated by natural killer cells. *J. Immunol. 149:581.*
3. Scalzo, A. A., P. A. Lyons, N. A. Fitzgerald, C. A. Forbes, W. M. Yokoyama, and G. R. Shellam. 1995. Genetic mapping of *Cmv1* in the region of mouse chromosome 6 encoding the NK gene complex-associated loci *Ly49* and mus*NKR-P1*. *Genomics 27:435.*
4. Forbes, C. A., M. G. Brown, R. Cho, G. R. Shellam, W. M. Yokoyama, and A. A. Scalzo. 1997. The *Cmv1* host resistance locus is closely linked to the *Ly49* multigene family within the natural killer cell gene complex on mouse chromosome 6. *Genomics 41:406.*
5. Brown, M. G., A. A. Scalzo, K. Matsumoto, and W. M. Yokoyama. 1997. The natural killer gene complex: a genetic basis for understanding natural killer cell function and innate immunity. *Immunol. Rev. 155:53.*
6. Azen, E. A., M. T. Davisson, M. Cherry, and B. A. Taylor. 1989. *Prp* (Proline-rich protein) genes linked to markers *Es-12* (Esterase-12), *Ea-10* (erythrocyte alloantigen), and loci on distal mouse chromosome 6. *Genomics 5:415.*
7. Yokoyama, W. M., P. J. Kehn, D. I. Cohen, and E. M. Shevach. 1990. Chromosomal location of the Ly-49 (A1, YE1/48) multigene family: genetic association with the NK 1.1 antigen. *J. Immunol. 145:2353.*
8. Yokoyama, W. M., J. C. Ryan, J. J. Hunter, H. R. Smith, M. Stark, and W. E. Seaman. 1991. cDNA cloning of mouse NKR-P1 and genetic linkage with Ly-49: identification of a natural killer cell gene complex on mouse chromosome 6. *J. Immunol. 147:3229.*
9. Brown, M. G., S. Fulmek, K. Matsumoto, R. Cho, P. A. Lyons, E. R. Levy, A. A. Scalzo, and W. M. Yokoyama. 1997. A 2-Mb YAC contig and physical map of the natural killer gene complex on mouse chromosome 6. *Genomics 42:16.*
10. Ho, E. L., J. W. Heusel, M. G. Brown, K. Matsumoto, A. A. Scalzo, and W. M. Yokoyama. 1998. Murine *Nkg2d* and *Cd94* are clustered within the natural killer complex and are expressed independently in natural killer cells. *Proc. Natl. Acad. Sci. USA 95:6320.*
11. Haldi, M. L., C. Strickland, P. Lim, V. VanBerkel, X. Chen, D. Noya, J. R. Korenberg, Z. Husain, J. Miller, and E. S. Lander. 1996. A comprehensive large-insert yeast artificial chromosome library for physical mapping of the mouse genome. *Mamm. Genome 7:767.*
12. Spencer, F., G. Ketner, C. Connelly, and P. Hieter. 1993. Targeted recombination-based cloning and manipulation of large DNA segments in yeast. *Methods 5:161.*
13. Birren, B., and E. Lai. 1993. *Pulsed Field Gel Electrophoresis: A Practical Guide*. Academic Press, Inc., San Diego.
14. Sambrook, J., E. F. Fritsch, and T. Maniatis. 1989. *Molecular Cloning: A Laboratory Manual*. Cold Spring Harbor Laboratory Press, Cold Spring Harbor, NY.
15. Dietrich, W., H. Katz, S. E. Lincoln, H. S. Shin, J. Friedman, N. C. Dracopoli, and E. S. Lander. 1992. A genetic map of the mouse suitable for typing intraspecific crosses. *Genetics 131:423.*
16. Scalzo, A. A., M. G. Brown, D. T. Chu, J. W. Heusel, W. M. Yokoyama, and C. A. Forbes. 1999. Development of intra-natural killer complex (NKC) recombinant and congenic mouse strains for mapping and functional analysis of NK cell regulatory loci. *Immunogenetics 49:238.*
17. Riley, J., R. Butler, D. Ogilvie, R. Finniear, D. Jenner, S. Powell, R. Anand, J. C. Smith, and A. F. Markham. 1990. A novel, rapid method for the isolation of terminal sequences from yeast artificial chromosome (YAC) clones. *Nucleic Acids Res. 18:2887.*

18. Dietrich, W., J. Miller, H. Katz, D. Joyce, R. Steen, S. Lincoln, M. Daly, M. P. Reeve, A. Weaver, P. Anagnostopoulos, N. Goodman, N. Dracopoli, and E. S. Lander. 1992. *Genetic Maps*. Cold Spring Harbor Laboratory Press, Cold Spring Harbor, NY.
19. Dietrich, W., J. Miller, H. Katz, D. Joyce, R. Steen, S. Lincoln, M. Daly, M. P. Reeve, A. Weaver, P. Anagnostopoulos, N. Goodman, N. Dracopoli, and E. S. Lander. 1992. *Genetic Map of the Mouse*. Whitehead Institute/MIT Center for Genome Research, Cambridge, MA.
20. Ann, D. K., and D. M. Carlson. 1985. The structure and organization of a proline-rich protein gene of a mouse multigene family. *J. Biol. Chem. 260:15863.*
21. McQueen, K. L., J. D. Freeman, F. Takei, and D. L. Mager. 1998. Localization of five new *Ly49* genes, including three closely related to *Ly49c*. *Immunogenetics 48:174.*
22. Depatie, C., E. Muise, P. Lepage, P. Gros, and S. M. Vidal. 1997. High-resolution linkage map in the proximity of the host resistance locus *Cmv1*. *Genomics 39: 154.*
23. Vance, R. E., J. R. Kraft, J. D. Altman, P. E. Jensen, and D. H. Raulet. 1998. Mouse CD94/NKG2A is a natural killer cell receptor for the nonclassical major histocompatibility complex (MHC) class I molecule Qa-1. *J. Exp. Med. 188: 1841.*
24. Delano, M. L., and D. G. Brownstein. 1995. Innate resistance to lethal mousepox is genetically linked to the NK gene complex on chromosome 6 and correlates with early restriction of virus replication by cells with an NK phenotype. *J. Virol. 69:5875.*
25. Idris, A. H., K. Iizuka, A. A. Scalzo, and W. M. Yokoyama. 1998. Genetic control of natural killing and in vivo tumor elimination by the *Chok* locus. *J. Exp. Med. 188:2243.*
26. Beebe, A. M., S. Mauze, N. J. Schork, and R. L. Coffman. 1997. Serial backcross mapping of multiple loci associated with resistance to *Leishmania major* in mice. *Immunity 6:551.*
27. Sudweeks, J. D., J. A. Todd, E. P. Blankenhorn, B. B. Wardell, S. R. Woodward, N. D. Meeker, S. S. Estes, and C. Teuscher. 1993. Locus controlling *Bordetella pertussis*-induced histamine sensitization (*Bphs*), an autoimmune disease-susceptibility gene, maps distal to T-cell receptor β-chain gene on mouse chromosome 6. *Proc. Natl. Acad. Sci. USA 90:3700.*
28. Melanitou, E., F. Joly, M. Lathrop, C. Boitard, and P. Avner. 1998. Evidence for the presence of insulin-dependent diabetes-associated alleles on the distal part of mouse chromosome 6. *Genome Res. 8:608.*
29. Dallas-Pedretti, A., M. McDuffie, and K. Haskins. 1995. A diabetes-associated T-cell autoantigen maps to a telomeric locus on mouse chromosome 6. *Proc. Natl. Acad. Sci. USA 92:1386.*
30. Suto, J., S. Matsuura, K. Imamura, H. Yamanaka, and K. Sekikawa. 1998. Genetic analysis of non-insulin-dependent diabetes mellitus in KK and KK-Ay mice. *Eur. J. Endocrinol. 139:654.*
31. Dissen, E., J. C. Ryan, W. E. Seaman, and S. Fossum. 1996. An autosomal dominant locus, *Nka*, mapping to the Ly-49 region of a rat natural killer (NK) gene complex, controls NK cell lysis of allogeneic lymphocytes. *J. Exp. Med. 183:2197.*
32. Capeless, C. G., G. Whitney, and E. A. Azen. 1992. Chromosome mapping of Soa, a gene influencing gustatory sensitivity to sucrose octaacetate in mice. *Behav. Genet. 22:655.*